Frequency Domain Identification of Acoustic Emission Events of Wood Fracture and Variable Moisture Content

Xinci Li
Ming Li
Shuang Ju

Abstract

The effect of moisture content on acoustic emission (AE) during wood damage was studied and the degree of damage was evaluated accordingly. In this article, the *Pinus massoniana* test-pieces of three different moisture content states, which are ovendried, air-dried, and water-saturated, were used to study the AE frequency characteristics of wood during bending failure. The original AE signal was subjected to wavelet denoising, and the denoised AE signal was classified into DAE (deformation AE) and FAE (fracture AE) according to the frequency distribution characteristics. Then, the instantaneous frequency of the AE signal was obtained by Hilbert transform, and the density of the two types of AE events was separately counted to evaluate the damage degree of the wood. The test results show that the AE signal in the process of wood damage and fracture was composed of two frequency components. The DAE signal frequency was concentrated at 30 to 60 kHz, the FAE signal was concentrated at 160 to 170 kHz, and the moisture content had no significant effect on the frequency distribution of AE events. In addition, the moisture content caused a change in the fracture toughness of the wood, so that the AE event density characteristics of the three damage processes were different. In particular, the ovendried test-piece showed obvious brittle fracture, and the AE event density level was slightly changed. Studies have shown that the change of AE event density based on instantaneous frequency can objectively evaluate and predict the degree of wood damage and fracture.

Acoustic emission (AE) is a phenomenon in which a material or structure is deformed or broken by an external force or an internal force to release strain energy in the form of an elastic wave. As the only active dynamic nondestructive testing method, acoustic emission technology (AET) has been widely used for defect detection of various materials such as metals, composite materials, and magnetic materials. In recent years, AET has gradually increased its application in the monitoring of wood damage and fracture to studying the differences of the crack propagation process between hardwood and softwood (Reiterer et al. 2000, Chen et al. 2006) and new and old wood (Ando et al. 2006) by some AE parameters such as amplitude, AE cumulative count, energy, etc.; to tracking breaks and defects in wooden cultural objects due to climate change in real time (Jakieła et al. 2008); to monitoring the damage of laminated timber and plywood during the stretching process (Ritschel et.al. 2013, 2014); to predicting the cracking position of wood-based materials by AE source localization (Niemz et al. 2009) and combined image acquisition method (Lamy et al. 2015); and to determining the crack initiation point of fiber/high-density polyethylene composite based on cumulative AE count (Guo et al. 2019). Existing research indicates that AET is also used for the identification of wood fracture patterns. The results of Wu et al. (2014) showed that the AE characteristics of wood cell wall fracture are high amplitude, high energy, and long duration, while the AE characteristics of cell wall damage and spallation, cell wall buckling, and collapse are low amplitude, low energy, and short duration. Choi et al. (2007) classified the AE signals of composite laminates by short-time Fourier transform into two types. The high-intensity, high-frequency band AE signals are generated by fiber breakage, and the low-frequency band AE signals are caused by matrix cracking or

The authors are, respectively, Master's Student, Professor, and Master's Student (1005054738@qq.com, swfu_lm@swfu.edu.cn [corresponding author], 2794045068@qq.com), School of Machinery and Transportation Engineering, Southwest Forestry Univ., Kunming, Yunnan, China. This paper was received for publication in June 2019. Article no. 19-00032.

Forest Prod. J. 70(1):107–114.
doi:10.13073/FPJ-D-19-00032

interface cracking. The abovementioned traditional AET for nondestructive monitoring of wood mostly uses the AE signal amplitude to evaluate the damage degree of wood. However, AE events cannot be objectively defined in the time domain on account of the influence of noise, but need to be defined and identified from the frequency domain. In comparison, the current research on the frequency domain analysis of AE signals for wood damage is still rare, and mainly focused on air-dried wood. In addition, AET is also used in new areas of wood testing: classification and performance prediction (Nasir et al. 2018, 2019c) of thermally modified wood; evaluation of adhesion of wood-carbon fiber composites (Rescalvo et al. 2018); and the monitoring of the presence and percentage of fines in particleboard ingredients (Campbell et al. 2018, Edwards et al. 2018). This also indicates that AET is an effective way to study the physical and mechanical properties of wood.

Existing studies have shown that the moisture content (MC) has a significant effect on the mechanical properties of wood (Hernández et al. 2014, Marcovich et al. 2015). It is clear that there are also differences in the characteristics of AE signals in wood damage and fracture at different MCs. Kang and Booker (2002) and Yamasaki et al. (2017) used the stress wave method to study the effect of MC on wave velocity. The results showed that the propagation velocity of stress wave decreases with the increase in MC. In addition, Yang et al. (2015) and Unterwieser (2011) studied the effect of MC on the ultrasonic acoustic properties of wood. Although the research on the influence of MC on the physical properties of wood has been extensive, there are few studies on the damage evolution process and mechanical behavior of wood using AET.

In this article, a method for identifying AE events of different fracture types in the frequency domain was proposed in view of the influence of MC on the characteristics of AE signals in the wood fracture process. The AE signal acquisition system was first used to collect the AE signal under three-point bending load. As a kind of nonstationary signal, the AE signal is susceptible to noise interference during the acquisition process. Therefore, the original AE signal was reconstructed by the discrete wavelet analysis method to achieve signal denoising, and AE events of different fracture types were defined based on the reconstructed signal. In order to obtain the frequency characteristics of the AE signal during the damage process in real time, the instantaneous frequency of the reconstructed AE signal was further obtained by Hilbert transform, and the density of the AE events of different fracture types was counted.

Materials and Methods

Experimental materials

Common *Pinus massoniana* Lamb was selected as the experimental material, and three test-pieces each having a size of 400 by 60 by 20 mm (length by width by thickness) were prepared and numbered T1, T2, and T3. First, the three test-pieces were dried in an oven at 103°C. Then, they were taken out every hour and immediately weighed with a YP B30002 electronic balance (Shanghai Guangzheng Medical Equipment Co., Ltd) until the weight was constant. The test-piece T1 was then placed in a sealed bag for use. The test-piece T2 was placed at room temperature of 25°C and relative humidity of 75 percent until the weight was constant. The test-piece T3 was immersed in water for about 1 week at room temperature of 25°C until the weight was constant, and the test-piece was placed in a sealed bag to ensure constant and uniform penetration of moisture. Among them, T1 is an ovendried test-piece, T2 is an air-dried test-piece, and T3 is a water-saturated test-piece.

The three-point bending tests for the test-pieces were carried out using a UTM5105 mechanical testing machine (Jinan Kason Testing Equipment Co., Ltd) at a loading speed of 1 mm/min and a span of 200 mm. Based on the NI USB-6366 high-speed acquisition card (National Instruments) and LabVIEW2013 software to build a two-channel AE signal acquisition system, the acquisition voltage amplitude of each channel was set to (–5 V, 5 V), sampling frequency was 500 kHz, and the maximum sampling frequency was 2 MHz. Existing research shows that the AE signal of wood is mainly distributed from 50 to 200 kHz, so the SR 150N single-resonance AE sensor was used, which operates from 22 to 220 kHz, and was equipped with a PAI preamplifier with a gain of 40 dB. During the test, two sensors were placed on the surface of the test-piece at a fixed distance of 300 mm (Fig. 1). In order to ensure that the sensor was fully coupled with the test-piece, vacuum silicone grease was applied between the test-piece and the sensor to reduce the influence of the air medium on the test results. In addition, a rubber band was used to hold the sensor against the surface of the test-piece to apply a constant pressure. The hardware composition of the entire test system is shown in Figure 2.

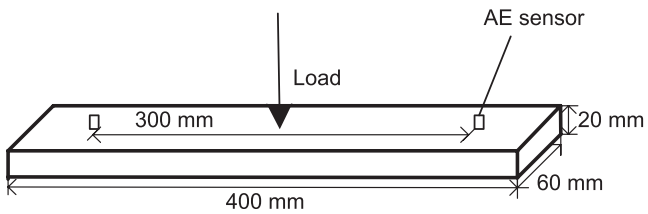

Figure 1.—Diagram of sensor arrangement. AE = acoustic emission.

Figure 2.—Hardware composition of three-point bending test. (a) Testing setup. (b) Acoustic emission equipment. (c) Air-dried test-piece.

AE signal processing method

The original signal collected was mixed with the ambient noise, so it was processed by the discrete wavelet transform method to reconstruct the AE signal waveform while realizing the signal denoising. The principle of wavelet denoising is to decompose the acquired signal and filter out the noise signal according to the difference between the noise and the effective signal under the discrete wavelet transform. The process of discrete wavelet transform is to decompose the signal level by level into approximation and detail coefficients, wherein the detail coefficients contain high-frequency components of the signal (Nasir et al. 2019a, 2019b). In this study, the AE signal was artificially added by the lead-core breaking method compared with the environmental noise signal, so the effective AE signal should be reflected in the high-frequency detail coefficient of wavelet decomposition. The Daubechies wavelet (db10) with higher vanishing moment order was selected as the wavelet basis function for 5-level wavelet decomposition. The sampling frequency of each channel is 500 kHz; therefore, it is theoretically possible to recognize signals in the range of 0 to 250 kHz. According to the principle of wavelet multiresolution analysis, from the first level, the detailed signal frequency range of each level of wavelet decomposition is (125 kHz, 250 kHz), (62.5 kHz, 125 kHz), (31.25 kHz, 62.5 kHz), (15.625 kHz, 31.25 kHz), (7.8125 kHz, 15.625 kHz). The frequency range of the SR 150N AE sensor is 22 to 220 kHz, so the 5-level wavelet decomposition can cover the effective frequency range of the sensor. A fixed threshold was defined according to the general threshold method, and the thresholding process was performed using a soft threshold method.

The wavelet denoised and reconstructed AE signal was decomposed into a series of intrinsic mode functions (IMF) by the empirical mode decomposition (EMD) algorithm. The IMF signal with the greatest correlation with the original signal was used as the final AE signal, and the instantaneous frequency was obtained. In order to obtain the instantaneous frequency of the AE signal, Hilbert transform was performed on the AE signal.

For any continuous time signal $X(t)$, its Hilbert transform $Y(t)$ is

$$Y(t) = \frac{1}{\pi} P \int_{-\infty}^{+\infty} \frac{X(\tau)}{t-\tau} d\tau \tag{1}$$

Constructing an analytical signal $Z(t)$ from the real signal $X(t)$ and its Hilbert transform $Y(t)$ is

$$Z(t) = X(t) + iY(t) = a(t)e^{i\theta(t)} \tag{2}$$

where $a(t)$ is the instantaneous amplitude and $\theta(t)$ is the phase.

$$a(t) = \left[X^2(t) + Y^2(t)\right]^{1/2}$$

$$\theta(t) = \arctan\left(\frac{Y(t)}{X(t)}\right) \tag{3}$$

The instantaneous frequency is calculated as follows:

$$\omega(t) = \frac{d\theta(t)}{dt} \tag{4}$$

Results and Discussion

Results and analysis of the three-point bending test

In this article, the test of three-point bending mechanics damage was carried out for the three moisture content test-pieces. In order to analyze the relationship between the stress and the AE event counts during the damage process of the test-pieces, the corresponding force–time curve was drawn (Fig. 3).

Time of the first macroscopic fracture of the ovendried, air-dried, and water-saturated test-pieces was about 323, 460, and 351 seconds, respectively (Fig. 3). Figure 4 shows the original AE signal waveform during the whole test. Compared with Figure 3 and Figure 4, the macroscopic fracture of the test-piece correspondingly produced a strong release of the AE signal. Especially in the ovendried and air-dried state, the test-piece had a very strong signal before the macroscopic fracture (Chen et al. 2006), indicating that damage had begun to appear inside the test-piece.

In addition, although the AE signal was obviously increased in the middle and late loading stages of the three kinds of test-pieces, it was not very dense. For example, a process of extremely small amplitude of AE signal occurred intermittently within the range of about 250 to 360 seconds in the ovendried test-piece, indicating that although the test-piece had a large fracture in the middle and late stages, it still had the ability to bear a certain load. In the later stages of the test, the fracture of the test-piece produced AE signals with large energy, so that the amplitude of the AE signal varied greatly throughout the test. Especially in the elastic deformation stage at the initial stage of loading, it was almost impossible to judge the occurrence of an AE event from the time domain waveform. Therefore, it was necessary to recognize the AE event from the frequency domain of the signal.

Discrete wavelet transform of AE signal

In order to obtain the characteristic frequency of the AE signal in the wood damage process, the original AE signal was decomposed and reconstructed to determine the type and characteristics of the AE signal. The sampling frequency of the signal was high, so it was difficult to directly process the whole signal. Therefore, when analyzing the characteristics of the AE signal, the data with a length of 10^4 (20 ms) were intercepted for discrete wavelet transform. First, the signal at the initial stage of loading was intercepted from 50 seconds for processing. The left half of

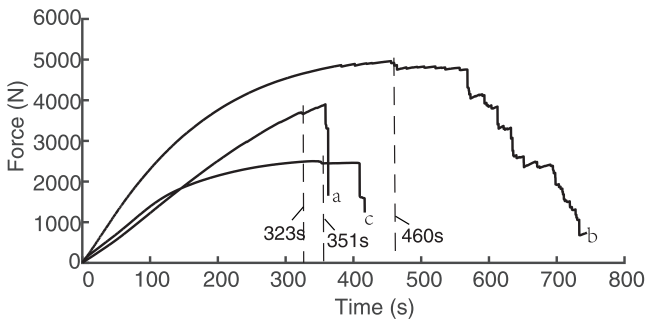

Figure 3.—Force–time curve of the three-point bending test. (a) Ovendried state. (b) Air-dried state. (c) Water-saturated state.

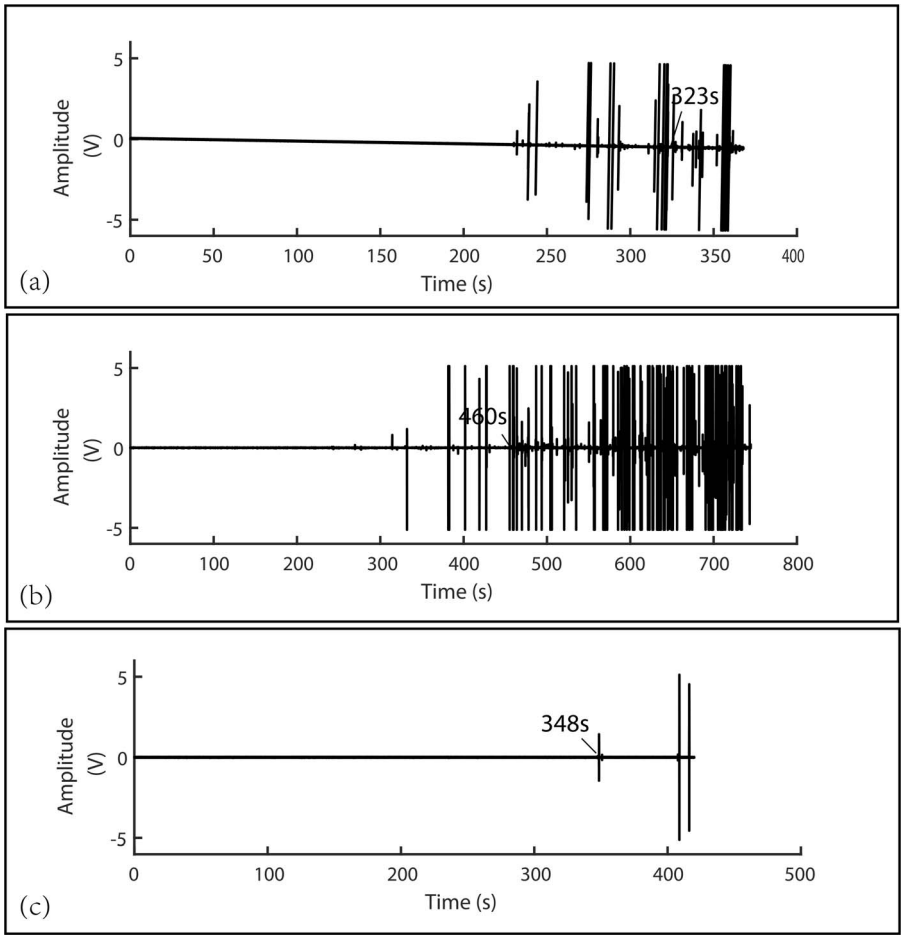

Figure 4.—Original acoustic emission signal waveform. (a) Ovendried state. (b) Air-dried state. (c) Water-saturated state.

Figure 5(5b, 5d, and 5f) shows the spectrum of the reconstructed AE signal at the beginning of the test. Then, data of 20 milliseconds were intercepted from 322.16 seconds at the loading time of the ovendried test-piece, 459.21 seconds at the loading time of the air-dried test-piece, and 408.83 seconds at the loading time of the water-saturated test-piece, respectively, because it can be seen from the time domain waveform that relatively strong AE signals were generated during this time. The right half of Figure 5(5b, 5d, and 5f) shows the spectrum of the reconstructed AE signal when the test-piece was strongly fractured.

There were two kinds of frequency components in the loading process of the test-piece (Fig. 5). In order to highlight the specific gravity of different frequency components, the amplitude of the signal spectrum was normalized. The amplitude of the AE signal at the initial stage of loading was relatively low, mainly distributed between 30 and 40 kHz. It could be considered that the deformation of the test-piece was caused by damage or delamination of cell wall of the wood. This type of signal was defined as a deformation AE (DAE) signal. The other type of AE signal was mainly concentrated around 165 kHz, corresponding to a larger amplitude. It could be considered a higher energy AE signal due to wood cell wall fracture, which was defined herein as a fracture AE (FAE) signal. When the ovendried and air-dried test-pieces were in the early stage of loading, the DAE signal they released was the main component. At this time, the FAE signal in reconstructed spectrum could be regarded as an AE signal generated by microcracks inside the test-piece. At the later stage of loading, FAE signal was the main signal, while DAE signal was the secondary component. However, DAE signal was the main signal in the loading process of the water-saturated test-piece, even in the period of obvious fracture. In the later stage of loading, the FAE signal was not obvious in the spectrogram because it was much smaller than the DAE signal.

Statistics of AE events

According to the previous analysis, the two types of AE signals appearing during the wood fracture process can be better distinguished by the signal frequency. In this article, the frequency range of the DAE event was set to (30 kHz, 60 kHz), and the frequency range of the FAE event was set to (160 kHz, 170 kHz). However, discrete wavelet analysis is still a global processing method, which can only distinguish the frequency components contained in the signal and cannot determine the frequency value of the signal at each moment. Therefore, after EMD was performed on the AE signal, the instantaneous frequency was obtained by Hilbert transform. In order to objectively reflect the AE events level of the test-piece during the damage process, the occurrence density of the two types of AE events was calculated at

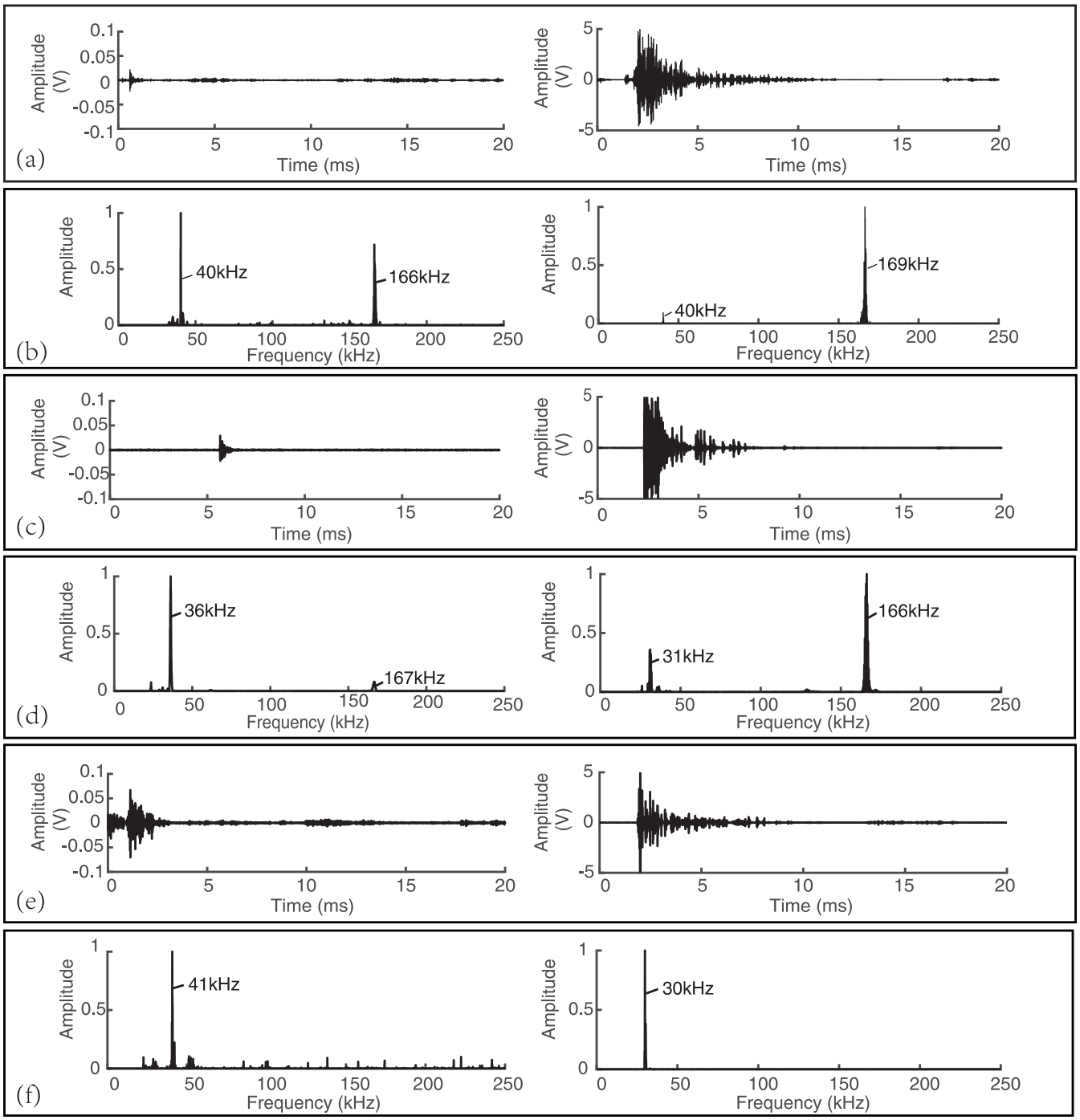

Figure 5.—Waveform and spectrum of acoustic emission (AE) signals based on wavelet reconstruction. (a) Waveform and (b) spectrum of AE signal reconstructed in the initial and late stages of the ovendried test-piece loading. (c) Waveform and (d) spectrum of AE signal reconstructed in the initial and late stages of the air-dried test-piece loading. (e) Waveform and (f) spectrum of AE signal reconstructed in the initial and late stages of the water-saturated test-piece loading.

intervals of 50 milliseconds according to the frequency range of the FAE and DAE determined in advance.

Figure 6 shows the density characteristics of two types of AE events during the entire loading process for the three MC test-pieces. The upper half is the density curve of the DAE events, and the lower half is the density curve of the FAE events. Density of DAE and FAE events were stable at a certain level in the case of the ovendried test-piece, with low stress in the early stage of the test (Fig. 6a). As the stress increased, microcracks appeared inside the test-piece and expanded continuously. Some very obvious AE events began to appear around 240 seconds, and the density of DAE and FAE events had a large, abrupt change, which indicates that the internal cracks of the test-piece increased, and the energy release also increased. In addition, both the DAE events and the FAE events could reflect the occurrence of internal fractures in the test-piece. When the loading time was around 350 seconds, the ovendried test-piece had a

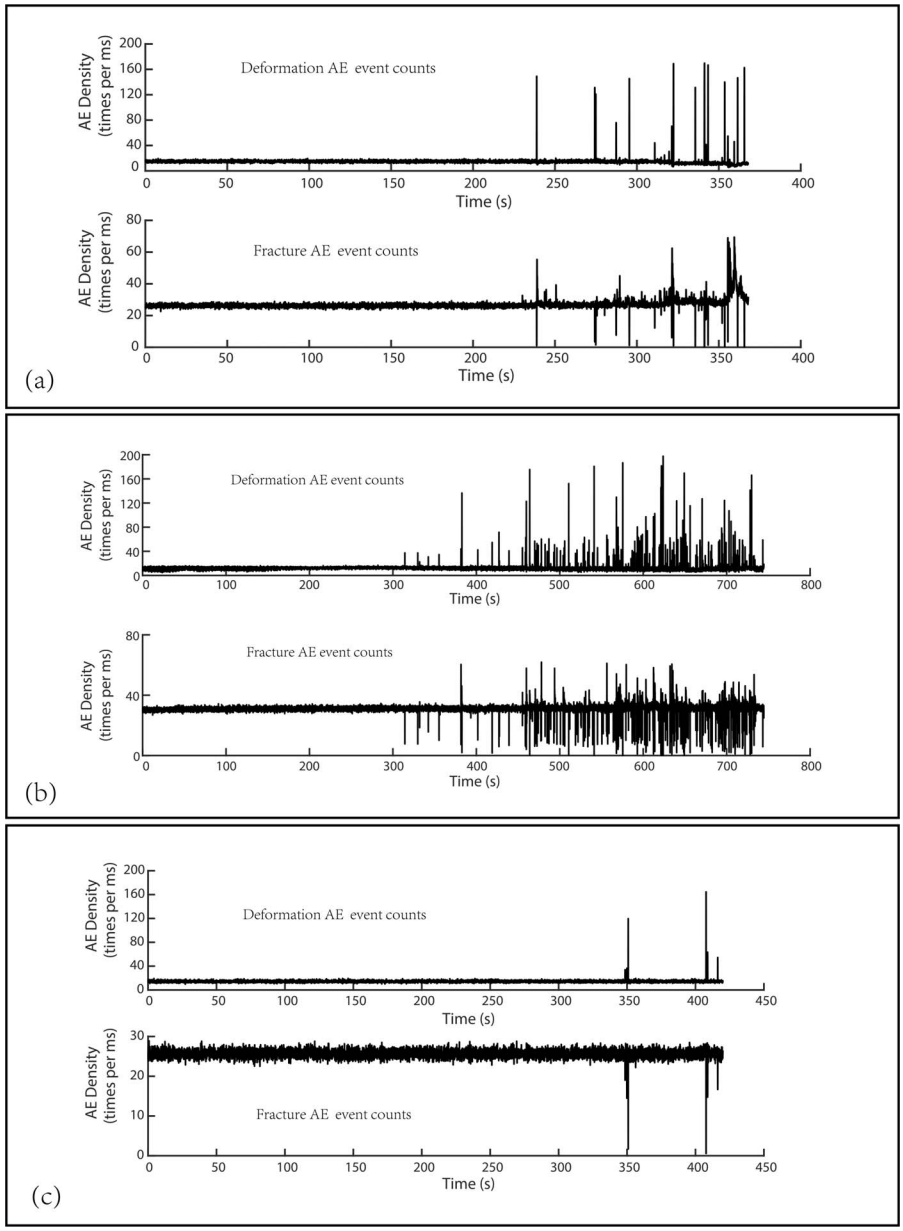

Figure 6.—Density of acoustic emission (AE) events. (a) Ovendried state. (b) Air-dried state. (c) Water-saturated state.

strong fracture and the density levels of the DAE events and the FAE events were slightly converted. The density level of the DAE events decreased slightly, and the density level of the FAE events increased significantly. This was consistent with the result of the complete fracture of the test-piece in Figure 3a around 350 seconds, indicating that the macroscopic fracture of the ovendried wood was mainly caused by the energy release of the cell wall fracture of the wood.

Figures 6b and 6c show the density curves of DAE and FAE events for air-dried and water-saturated test-pieces, respectively. Different from the test results of the ovendried test-piece, these two did not have obvious conversion in the density level of DAE and FAE events. In addition, the test of the air-dried test-piece lasted a long time, so the stress release was relatively more sufficient in the three test-pieces, which is related to the influence of MC on the fracture toughness of the wood (Ewing and Williams 1979). In general, the wood in the ovendried state is enhanced in brittleness and relatively low in toughness, and suddenly fractures without significant plastic deformation. Therefore, the brittle fracture occurred mainly in the ovendried test-piece, and the duration of the damage and fracture process was significantly shortened compared with the air-dried test-piece. The number of abrupt changes in the density of the DAE events or the FAE events of the saturated test-piece were significantly reduced (Fig. 6c), indicating that the stress release level of the water-saturated test-piece during the damage process was also significantly lower. In fact, the water-saturated test-piece was not noticeable macroscopically throughout the test, except that there was a slight crack on the surface. In addition, as the stress increased, the moment at which the density of the DAE event was concentrated substantially corresponded to the FAE event (Fig. 6), indicating that the two types of AE signals existed

simultaneously during the fracture of the test-piece. The abrupt density changes of DAE events in ovendried and air-dried test-pieces were above the density evaluation level each time, while the abrupt density changes of FAE events were basically below the density evaluation level, except when the test-pieces showed strong fractures. This means that the crack initiation and propagation in the test-piece were accompanied by large elastic deformation until the macroscopic fracture. However, the fracture of the water-saturated test-piece was inconspicuous, so the elastic deformation was the main part in the whole test process.

Conclusion

It is difficult to effectively distinguish different AE signals based on time domain waveform. However, the frequency domain characteristics of the signals can better distinguish different types of AE signals. Based on the experimental research, the AE signal generated by wood in the process of damage was divided into two types according to its frequency distribution characteristics—one is the lower frequency DAE signal, and the other is the relatively high-frequency FAE signal. The degree of density change of the two types of AE events can objectively reflect the crack formation process and stress state of the test-piece. Although the MC in the three test-pieces was different, the frequency distribution ranges of the DAE signal and the FAE signal were the same. This indicates that the MC has no significant effect on the frequency characteristics of the AE signal of wood damage and fracture.

MC has a direct effect on the mechanical properties of wood, which leads to differences in the release of AE signals when MC is different. This difference can be explained from the perspective of the effect of MC on fracture toughness of wood. The air-dried test-piece has the best fracture toughness, and the fracture process needs to release more energy, which is manifested by more AE signal generation for a longer period of time. The toughness of the ovendried and water-saturated test-pieces is relatively poor, and it can be considered that brittle fracture occurs. This fracture process consumes relatively little energy, but typically produces an extremely intense energy release in an instant, which is manifested as a conversion of the AE event density level in the ovendried test piece.

In addition, the degree of abrupt change in the density of FAE events reflects the intensity of the fracture, and the number of abrupt changes reflects the frequency of occurrence of stronger fracture. The number of abrupt changes of DAE and FAE events in the three test-pieces increased significantly in the middle and late stages of the test. Among them, the abrupt density changes of the two AE events in the air-dried test-piece were the most frequent, followed by the ovendried test-piece, and finally the water-saturated test-piece. Wood with different MC and its degree of damage can be distinguished according to the number of abrupt changes in the density of AE events.

Acknowledgment

Part of this research was funded by China Natural Science Foundation (NO: 31760182).

Literature Cited

Ando, K., Y. Hirashima, M. Sugihara, H. Sakiko, and S. Yasutoshi. 2006. Microscopic processes of shearing fracture of old wood, examined using the acoustic emission technique. *J. Wood Sci*. 52(6):483–489.

Campbell, L., K. Edwards, R. Lemaster, and G. Velarde. 2018. The use of acoustic emission to detect fines for wood-based composites, part one: Experimental setup for use on particleboard. *BioResources* 13(4):8738–8750.

Chen, Z., B. Gabbitas, and D. Hunt. 2006. Monitoring the fracture of wood in torsion using acoustic emission. *J. Mater. Sci*. 41(12):3645–3655.

Choi, N. S., S. C. Woo, and K. Y. Rhee. 2007. Effects of fiber orientation on the acoustic emission and fracture characteristics of composite laminates. *J. Mater. Sci*. 42(4):1162–1168.

Edwards, K., L. Campbell, R. Lemaster, and G. Velarde. 2018. The use of acoustic emission to detect fines for wood based composites, part two: Use on flakes. *BioResources* 13(4):8751–8760.

Ewing, P. D. and J. G. Williams. 1979. Thickness and moisture content effect in the fracture toughness of Scots Pine. *J. Mater. Sci*. 14(12):2959–2966.

Guo, Y., S. Zhu, Y. Chen, D. Liu, and D. Li. 2019. Acoustic emission-based study to characterize the crack initiation point of wood fiber/HDPE composites. *Polymers* 11(4):701. DOI:https://doi.org/10.3390/polym11040701

Hernández, R. E., L. Passarini, and A. Koubaa. 2014. Effects of temperature and moisture content on selected wood mechanical properties involved in the chipping process. *Wood Sci. Technol*. 48(6):1281–1301.

Jakieła, S., Ł. Bratasz, and R. Kozłowski. 2008. Acoustic emission for tracing fracture intensity in lime wood due to climatic variations. *Wood Sci. Technol*. 42(4):269–279.

Kang, H. and R. E. Booker. 2002. Variation of stress wave velocity with MC and temperature. *Wood Sci. Technol*. 36(1):41–54.

Lamy, F., M. Takarli, N. Angellier, F. Dubois, and O. Pop. 2015. Acoustic emission technique for fracture analysis in wood materials. *Int. J. Fract*. 192(1):57–70.

Marcovich, N. E., M. M. Reboredo, and M. I. Aranguren. 2015. Dependence of the mechanical properties of woodflour–polymer composites on the moisture content. *J. Appl. Polym. Sci*. 68(13):2069–2076.

Nasir, V., J. Cool, and F. Sassani. 2019a. Acoustic emission monitoring of sawing process: Artificial intelligence approach for optimal sensory feature selection. *Int. J. Adv. Manuf. Technol*. 102(9–12):4179–4197.

Nasir, V., J. Cool, and F. Sassani. 2019b. Intelligent machining monitoring using sound signal processed with the wavelet method and a self-organizing neural network. *IEEE Robot. Autom. Mag. Lett*. 4(4):3449–3456.

Nasir, V., S. Nourian, S. Avramidis, and J. Cool. 2018. Stress wave evaluation by accelerometer and acoustic emission sensor for thermally modified wood classification using three types of neural networks. *Eur. J. Wood Wood Prod*. DOI:https://doi.org/10.1007/s00107-018-1373-1

Nasir, V., S. Nourian, S. Avramidis, and J. Cool. 2019c. Stress wave evaluation for predicting the properties of thermally modified wood using neuro-fuzzy and neural network modeling. *Holzforschung* 73(9):827–838.

Niemz, P., A. J. Brunner, and O. Walter. 2009. Investigation of the mechanism of failure behaviour of wood based materials using acoustic emission analysis and image processing. *Wood Res*. 54(2):49–62.

Reiterer, A., S. E. Stanzl-Tschegg, and E. K. Tschegg. 2000. Mode I fracture and acoustic emission of softwood and hardwood. *Wood Sci. Technol*. 34(5):417–430.

Rescalvo, F. J., A. Aguilar-Aguilera, E. Suarez, I. Valverde-Palacios, and A. Gallego. 2018. Acoustic emission during wood-CFRP adhesion tests. *Int. J. Adhes. Adhes*. 87:79–90. DOI:https://doi.org/10.1016/j.ijadhadh.2018.09.007

Ritschel, F., A. J. Brunner, and P. Niemz. 2013. Nondestructive evaluation of damage accumulation in tensile test specimens made from solid wood and layered wood materials. *Compos. Struct*. 95(1):44–52.

Ritschel, F., Z. Yang, A. J. Brunner, T. Fillbrandt, and P. Niemz. 2014. Acoustic emission analysis of industrial plywood materials exposed to destructive tensile load. *Wood Sci. Technol*. 48(3):611–631.

Unterwieser, H. 2011. Influence of moisture content of wood on sound

velocity and dynamic MOE of natural frequency- and ultrasonic runtime measurement. *Eur. J. Wood Wood Prod*. 69(2):171–181.
Wu, Y., Z. P. Shao, F. Wang, and G. L. Tian. 2014. Acoustic emission characteristics and felicity effect of wood fracture perpendicular to the grain. *J. Trop. Forest Sci*. 26(4):522–531.
Yamasaki, M., C. Tsuzuki, Y. Sasaki, and Y. Onishi. 2017. Influence of moisture content on estimating Young's modulus of full-scale timber using stress wave velocity. *J. Wood Sci*. 63(3):225–235.
Yang, H., Y. Lei, and L. Wang. 2015. Effect of moisture content on the ultrasonic acoustic properties of wood. *J. Forest Res*. 26(3):753–757.